

Experiments on the stability of convection rolls in fluids whose viscosity depends on temperature

By FRANK M. RICHTER

Department of the Geophysical Sciences, University of Chicago, Illinois 60637

(Received 31 October 1977 and in revised form 1 May 1978)

The stability of two-dimensional convection rolls has been studied as a function of the Rayleigh number, wavenumber and variation in viscosity. The experiments used controlled initial conditions for the wavenumber, Rayleigh numbers up to 25 000 and variations in viscosity up to a factor of about 20. The parameter range of stable rolls is bounded by a hexagonal-cell regime at small Rayleigh numbers and large variations in viscosity. Otherwise, the rolls are subject to the same transitions as have already been studied in fluids of uniform viscosity. The bimodal instability leading to a stable three-dimensional pattern occurs at smaller values of the average Rayleigh number as the variations in viscosity increase. This appears to be a consequence of the low viscosity of the warm thermal boundary layer associated with the original rolls.

1. Introduction

The experiments discussed below are an attempt to begin to understand the effect of temperature-dependent viscosity on the spatial structure of convection. The effects of large viscosity variations are particularly important to convection models applied to planetary interiors, where the ease of deformation is known to be a strong function of temperature (see McKenzie, Roberts & Weiss 1974). There is also the more general motivation of determining to what extent variations in viscosity modify previous results for Boussinesq fluids.

Earlier studies with large variations in viscosity have consisted of two-dimensional numerical simulations (Torrance & Turcotte 1971) or laboratory experiments determining the relation between the Rayleigh number and the Nusselt number (Booker 1976). The numerical studies, being limited to two dimensions, do not address the issue of which planforms are realizable. The laboratory experiments on the heat-transfer efficiency of a variable-viscosity fluid find that the relation between the Rayleigh number and the Nusselt number is not much different from that of a uniform-viscosity fluid if the viscosity used to calculate the Rayleigh number is the viscosity corresponding to the average temperature of the layer. I shall call the Rayleigh number defined in this way the average Rayleigh number \bar{R}_a :

$$\bar{R}_a = g\alpha\Delta T D^3 / \kappa\nu_{\bar{T}}, \quad \bar{T} = \frac{1}{2}(T_1 + T_2), \quad \Delta T = T_2 - T_1,$$

where g is the acceleration due to gravity, α is the coefficient of thermal expansion, D is the depth, κ is the thermometric diffusivity, $\nu_{\bar{T}}$ is the viscosity when the temperature T equals \bar{T} , T_1 is the temperature at the top of the convecting layer and T_2 is the temperature at the bottom.

In contrast to the earlier work, the present study emphasizes the planform of finite amplitude convection. The experiments use controlled initial conditions to investigate the stability of two-dimensional rolls as a function of the Rayleigh number, wavenumber and degree of variation of the viscosity. The experimental design and methods are very similar to those used by Busse & Whitehead (1971) for a similar study of convection in a uniform-viscosity fluid. The only new planform seen as a result of the variation in viscosity is a hexagonal one that occurs at small Rayleigh number and large viscosity variation. With increasing Rayleigh number the hexagonal planform transforms to rolls and thereafter the planforms are virtually indistinguishable from those reported by Busse & Whitehead, despite viscosity variations in the present experiments as large as a factor of twenty. The only significant quantitative difference is that the bimodal instability, which represents the transition of rolls to a stable three-dimensional flow, occurs at lower values of \bar{R}_a in the variable-viscosity fluid. There is no evidence of a broader band of wavenumbers being stable as a consequence of the variation of viscosity with temperature.

The experimental design and methods, as well as the properties of the fluids used, are given in § 2. A summary of the results is given in § 3, followed by a brief discussion.

2. Experimental design and procedure

The experiments are designed with two principal criteria in mind: the ability to establish controlled initial conditions and the subsequent observation of the convective planforms. The convection tank is built of $\frac{1}{4}$ in. glass. The temperature on the horizontal boundaries of the convecting region is controlled by water of regulated temperature flowing in thin water channels formed by superimposed plates of glass, as shown in figure 1. The characteristic horizontal dimension of the convecting region is 1 m compared with a depth always less than 3 cm. The depth is determined by removable spacers between the upper and lower water channels. The water pressures must be controlled by constant-level spillways in order to minimize the bending of the glass plates due to differential pressures. In the process of accurately levelling the tank the bowing of the glass can be measured as a function of the differential pressure, and with some care the variations in depth can be reduced to ± 0.15 mm. The uniformity of the temperature on the horizontal boundaries depends on both the constancy of the temperatures of the water sources and the flow rate. The temperatures of the water sources are constant to within ± 0.01 °C over the duration of an experiment, which can be as long as 12 h. The horizontal variations in temperature due to the heat flux into the water channels can be as large as 0.2 °C for a flow rate of 40 l min⁻¹. This variation can be reduced by increasing the flow rate but the accompanying larger pressure gradients cause further bowing of the glass plates. A flow rate of 40 l min⁻¹ seems the best compromise. The overall design and characteristic dimensions are as similar as possible to those used by Busse & Whitehead (1971) to allow the direct comparison of results. The Prandtl number of the fluids used in the present experiments is about 10³, which is an order of magnitude greater than that of the fluid used by Busse & Whitehead.

The experiments were carried out using two different fluids: 99% pure glycerine and L100 polybutene oil provided by the Amoco Chemical Company. The variation of viscosity with temperature of these fluids is shown in figure 2. A range in \bar{R}_a of up

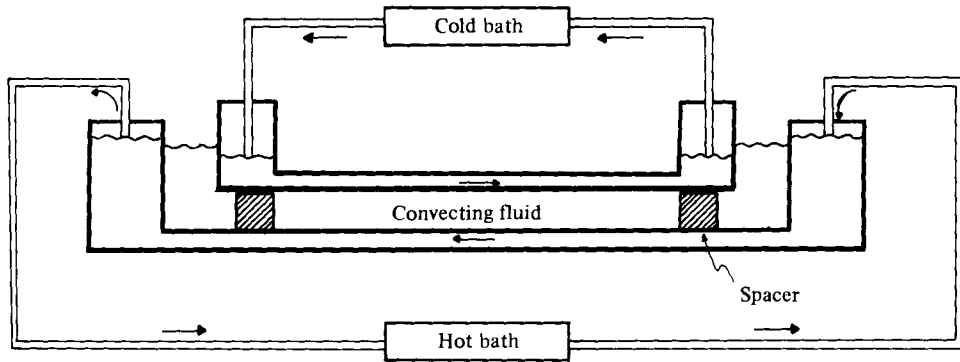


FIGURE 1. Schematic cross-section of the convection apparatus. The characteristic horizontal dimensions of the convecting region are about 1 m compared with depths of 2.81, 1.92, 1.79 and 1.28 cm. The tanks are made out of glass to allow observation of the planforms.

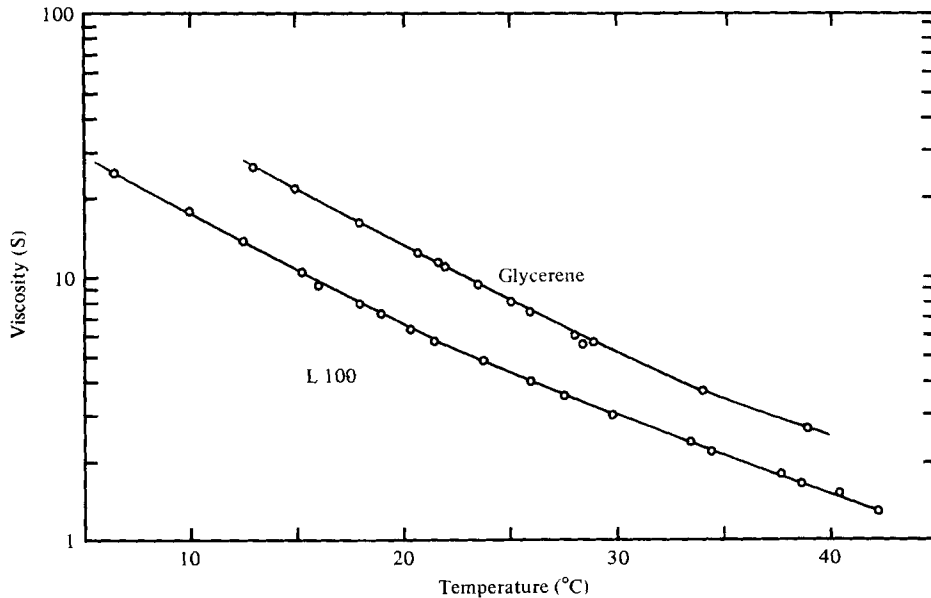


FIGURE 2. Viscosity of 99% pure glycerine and L100 polybutene oil as a function of temperature.

to 25000 and a maximum variation in viscosity (ν_{\max}/ν_{\min}) of greater than 20 was achieved by varying the depth ($D = 2.81, 1.92, 1.79$ and 1.28 cm) and mean temperature ($\bar{T} = 20, 25$ and 30 °C). The reported values of the coefficient of expansion and thermometric diffusivity of the fluids used are not generally reliable. For this reason, and also to account to a first approximation for the effect of the glass boundaries, the reported values of \bar{R}_a are based on the definition

$$\bar{R}_a = 1707 \Delta T / \Delta T_c,$$

where 1707 is the theoretical value of the critical Rayleigh number for a uniform-viscosity fluid between rigid isothermal boundaries, ΔT_c is the measured critical

temperature difference between the water sources for the onset of convection, and ΔT is the temperature difference between the water sources for each experiment. ΔT_c was measured for each fluid, depth and mean temperature used in subsequent experiments. A measure of the accuracy with which ΔT_c was determined was obtained by repeatedly crossing the stability boundary and also by comparing the different values of ΔT_c for each fluid after the effect of depth, mean temperature and temperature drop across the glass boundaries had been accounted for. The largest differences in ΔT_c ($\sim 8\%$) are for the experiments using glycerine, which can become stably stratified owing to density variations associated with changes in water concentration as small as 0.1%. It will be seen that errors of even 10% in \bar{R}_a are not significant in terms of the present purposes of the experiments.

The reported Rayleigh numbers are not exact for other reasons. The value 1707 used in the operational definition of \bar{R}_a is really appropriate only for a uniform-viscosity fluid between isothermal boundaries. The glass boundaries will reduce the critical Rayleigh number by several per cent (Nield 1968). This effect is of little consequence given the other, much larger sources of uncertainty. The variation in viscosity in the experiments for ΔT_c is sufficiently small to have a negligible effect on the critical Rayleigh number. The most important difference between the reported and the actual Rayleigh number will be due to the increased proportional temperature drop across the glass boundaries as convection becomes more vigorous. The present definition of \bar{R}_a accounts for the temperature drop across the glass only in the case of quiescent fluid. For Nusselt numbers greater than one, the temperature drop across the glass will have been underestimated and the reported Rayleigh numbers will be too large. The relationship between the Rayleigh number and the Nusselt number required to correct \bar{R}_a has not been determined in the relevant parameter range and therefore it seems preferable to omit any further correction. The reported Rayleigh numbers near the critical value require no correction, while the highest reported Rayleigh numbers may be too large by as much as 15%.

The investigation of the stability of two-dimensional rolls requires controlled initial conditions. The method of Chen & Whitehead (1968) has been used. In order to induce a desired wavenumber the fluid layer is held at a subcritical temperature gradient while periodic temperature perturbations of the desired wavelength are imposed by shining two 600 W lamps through a grid and onto the convecting layer. The perturbations are induced for a length of time equal to the thermal diffusion time D^2/κ ($\kappa \sim 10^{-3}$ cm²/s for both fluids). The desired \bar{R}_a is then achieved by changing the temperatures of the cold and the warm water sources at the same rate. Once the desired \bar{R}_a is reached the lamps and grid are removed and the planform is observed by use of a shadowgraph technique. The shadowgraph is produced by shining a weak, slightly divergent beam of light vertically through the convecting layer and then projecting it onto a frosted screen. Regions of predominantly warm, rising fluid appear as dark areas on the screen while cold, sinking regions show up as light areas. The shadowgraph gives an impression of the planform that is straightforward in the case of two-dimensional rolls. Parallel light and dark bands are seen. In the case of three-dimensional flows the pattern can be very complex owing to the averaging over the entire depth of the fluid. Light and dark areas often intersect, indicating that both warm and cold fluid are superimposed, but providing no further information. This method of visualization is crude, but adequate for present purposes.

Once the two-dimensional convective planform has been established as an initial condition, an operational definition of its stability must be given. If a planform is essentially unchanged after five thermal diffusion times ($t > 5D^2/\kappa$) it is considered stable. The meaning of 'essentially unchanged' is of course subjective, but the long observation times minimize its practical importance.

3. Experimental results

Two-dimensional convection rolls in a variable-viscosity fluid are seen to be subject to four types of transition:

(i) The transition to a hexagonal planform that occurs at a small Rayleigh number and large variation in viscosity.

(ii) The zigzag instability that transforms rolls of too small a wavenumber into a new set of rolls of larger and stable wavenumber.

(iii) The cross-roll instability that transforms rolls of too large a wavenumber into a new set of rolls at right angles with a smaller and thus stable wavenumber.

(iv) The bimodal instability, which represents the transition to a three-dimensional planform, occurs with increasing Rayleigh number and leads to two sets of rolls at right angles coexisting stably.

Examples of these four transitions are given in figures 3 and 4 (plates 1 and 2). The zigzag, cross-roll and bimodal instabilities shown in figure 4 (plate 2) are indistinguishable from the instabilities reported by Busse & Whitehead (1971) for a fluid of uniform viscosity. The existence of a hexagonal planform is due to the variation in viscosity with temperature. The transition between hexagons and rolls was not studied in detail, but enough cases were run to suggest that the transition depends to a large degree on the perfection of the hexagonal pattern. Flawed hexagons transform readily to rolls while perfect hexagons are very resistant to change. This causes great difficulty in the experiments determining the transition because any hexagonal pattern will be flawed where it meets the vertical boundaries of the apparatus, and will have a tendency to transform to rolls there first. A further difficulty is that both hexagons and rolls may in fact be stable at the same point in parameter space, and which are realized depends on the initial conditions. At Rayleigh numbers less than twice the critical value and variations in viscosity of about a factor of ten, hexagons or rolls can persist essentially unchanged for periods of time greater than twenty thermal diffusion times ($t > 20D^2/\kappa$).

The three other transitions were studied systematically in order to map out the parameter space of stable two-dimensional rolls. Experiments with variations in viscosity ranging from a factor of 2.5 to a factor of 6 have been plotted together in figure 5. The solid curves bound the theoretically determined stability field of rolls in a uniform-viscosity fluid (Busse 1967) and are included in the figure only to make it easier to compare these results with those of Busse & Whitehead (1971). The dashed curve is the approximate boundary found in the present experiments, and differs from the theoretical curves by being shifted slightly towards smaller wavenumbers and by closing at smaller values of the average Rayleigh number. This figure can be compared with the corresponding figure given by Busse & Whitehead (1971, figure 6) for experiments on a uniform-viscosity fluid. They found a similar shift of the stability boundaries to smaller wavenumbers and attributed it to the effect of the horizontal

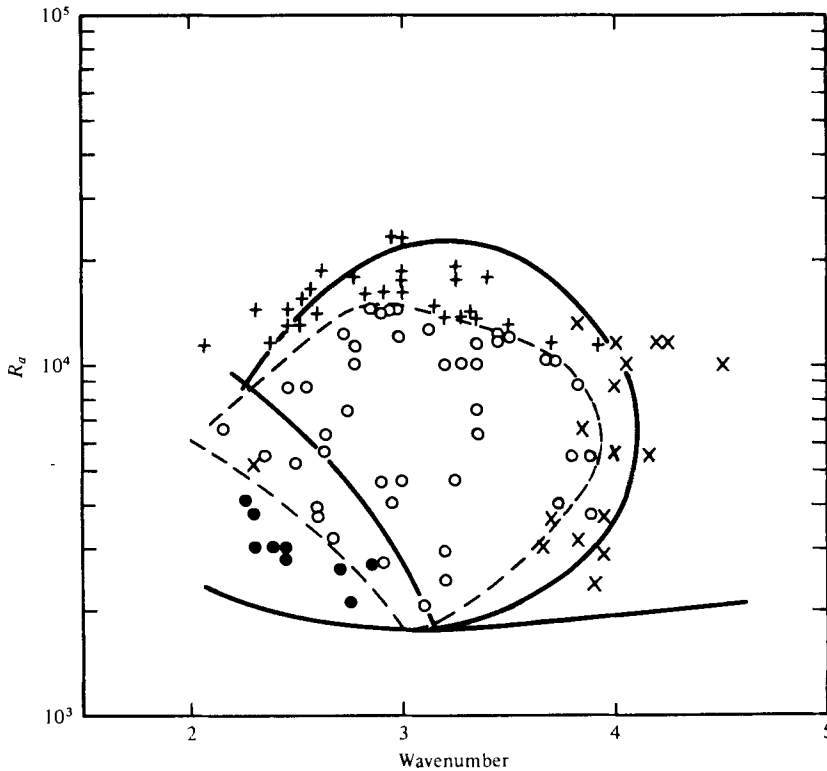


FIGURE 5. Experimental results for ν_{\max}/ν_{\min} in the range 2.5–6.0. \circ , stable rolls; \bullet , zig-zag instability; \times , cross-roll instability; $+$, bimodal convection. The solid curves bound the theoretical region of stable rolls for a uniform-viscosity fluid found by Busse (1967). The dashed curves form an approximate boundary for the region of stable rolls found in the present experiments.

glass boundaries. Such an interpretation is consistent with the effect of the glass boundaries on the critical wavenumber found in the linear theory (Nield 1968). Within the accuracy of both sets of experiments, there is no indication that variations in viscosity as large as a factor of six cause any tendency for a broader band of wavenumbers to be realized at finite amplitude.

The lowering of the average Rayleigh number at the top of the stable roll region is clearer in figure 6. The solid-line segments join the highest Rayleigh number at which rolls are still stable to the lowest Rayleigh number at which bimodal convection occurs in a given set of experiments in which the Rayleigh number was raised in small increments. The length of each segment provides a measure of the accuracy to which the transition is determined. Only those experiments with wavenumbers in the range 2.9–3.2 are included in the figure in an effort to remove the effect of the wavenumber on the transition. Two different definitions of the Rayleigh number have been used in plotting the data. The lower data points, which tend towards smaller values as the variation in viscosity increases, are plotted using \bar{R}_a as defined earlier. In terms of \bar{R}_a the bimodal transition occurs at a significantly smaller Rayleigh number than in a uniform-viscosity fluid, for which Busse & Whitehead (1971) report stable rolls with a Rayleigh number equal to 20 000. Data from both glycerine and polybutene oil are included in the figure. The good agreement between similar cases

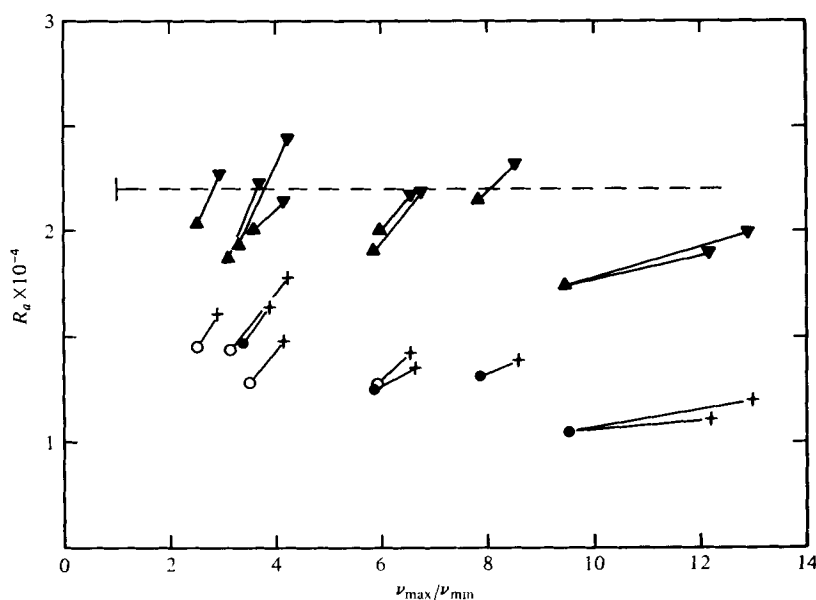


FIGURE 6. Experimental results for the bimodal transition as a function of ν_{\max}/ν_{\min} plotted using two different definitions of the Rayleigh number. The line segments join the largest Rayleigh number at which rolls are still stable to the lowest Rayleigh number for bimodal convection in experiments with initial wavenumber in the range 2.9–3.2. \circ , rolls in glycerine; \bullet , rolls in L100; +, bimodal convection in either glycerine or L100. These symbols are used to plot results as a function of \bar{R}_a (the Rayleigh number defined using the viscosity at the mean temperature of the layer). The symbols \blacktriangle and \blacktriangledown represent the same rolls and bimodal convection but now plotted using \tilde{R}_a (the Rayleigh number based on an estimate of the viscosity of the warm thermal boundary layer). \bar{R}_a and \tilde{R}_a are defined in the text. The dashed line shows the theoretical Rayleigh number for the bimodal transition in a uniform-viscosity fluid.

using different fluids gives confidence that the results are due to the variation in viscosity with temperature and not to some other effect such as the contamination of glycerine with water.

The bimodal transition is due to an instability of the thermal boundary layers of the original rolls and therefore the Rayleigh number based on the average viscosity of the entire layer overestimates the stability of the low viscosity thermal boundary layer. A Rayleigh number taking into account the local properties of the lower thermal boundary layer can be defined as

$$\tilde{R}_a = \bar{R}_a \nu_{\bar{T}}/\nu_{bl},$$

where $\nu_{\bar{T}}$ is the viscosity at the average temperature of the entire layer and ν_{bl} is the viscosity at a temperature $T_{bl} = \frac{1}{2}(\bar{T} + T_2)$, which should be a good approximation to the average temperature of the lower boundary layer. When the data in figure 6 are plotted using \tilde{R}_a , the transition occurs at a more constant value of the Rayleigh number, which is now closer to the value of 20 000 found in experiments with uniform-viscosity fluids. This seems to confirm that in a variable-viscosity fluid the bimodal transition results from the instability of the thermal boundary layer with lower viscosity. It is somewhat surprising then that the bimodal pattern is not different from that seen in a uniform-viscosity fluid, in which both thermal boundary layers are equally unstable. The characteristic wavenumber of the new set of rolls is very

similar to that seen in a uniform-viscosity fluid. Even the streamlines do not appear to be different. Figure 7 (plate 3) is an enlargement of a very weak bimodal pattern. The goblet-shaped streaks represent streamlines that are consistent with the interpretation of the bimodal flow as a superposition of two sets of rolls at right angles. In this particular experiment, the cold thermal boundary layer should still be stable, yet the streamlines are very similar to those seen or expected in the uniform-viscosity case (see figures 3 and 8 of Busse & Whitehead 1971).

4. Conclusions

Several general conclusions can be drawn from the experiments. The most striking is that apart from the hexagonal pattern the observed planforms are indistinguishable from those in a uniform-viscosity fluid despite viscosity variations larger than an order of magnitude. The only obvious difference due to the variation in viscosity with temperature is the lowering of the average Rayleigh number for the bimodal transition with increasing variation in viscosity. It was argued that this result is due to the greater tendency towards instability of the low viscosity thermal boundary layer at the base of the convecting region.

I am grateful to Dave Fultz for advice and for the use of the facilities in the Hydrodynamics Laboratory of the University of Chicago. Robert White helped to build the convection apparatus. The Amoco Chemical Company kindly provided the polybutene oil used in some of the experiments. This research was supported by the National Science Foundation, Grant number NSF EAR75-17170.

REFERENCES

- BOOKER, J. 1976 *J. Fluid Mech.* **76**, 741.
BUSSE, F. H. 1967 *J. Math. & Phys.* **46**, 140.
BUSSE, F. H. & WHITEHEAD, J. A. 1971 *J. Fluid Mech.* **47**, 305.
CHEN, M. M. & WHITEHEAD, J. A. 1968 *J. Fluid Mech.* **31**, 1.
MCKENZIE, D. P., ROBERTS, J. M. & WEISS, N. O. 1974 *J. Fluid Mech.* **62**, 465.
NIELD, D. A. 1968 *J. Fluid Mech.* **32**, 393.
TORRANCE, K. E. & TURCOTTE, D. L. 1971 *J. Fluid Mech.* **47**, 113.

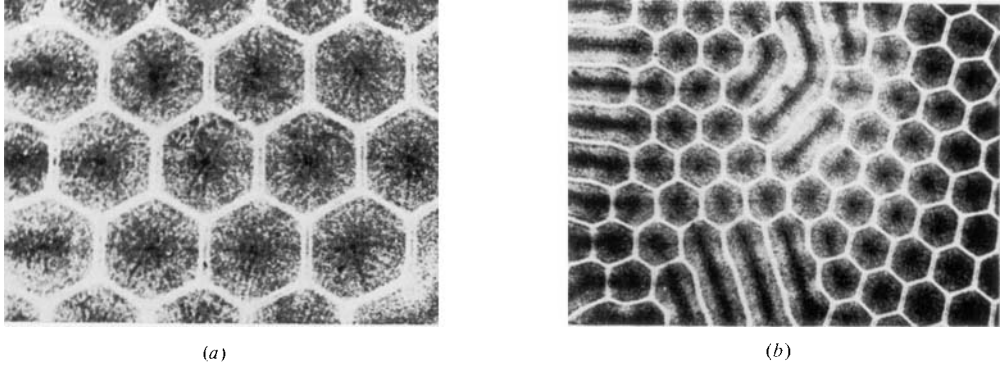


FIGURE 3. (a) Shadowgraph of hexagonal cells with upwelling in the centre of each cell at $\bar{R}_a = 2460$, $\nu_{\max}/\nu_{\min} = 7$. (b) Hexagons transforming to rolls at $\bar{R}_a = 3850$, $\nu_{\max}/\nu_{\min} = 13.7$.

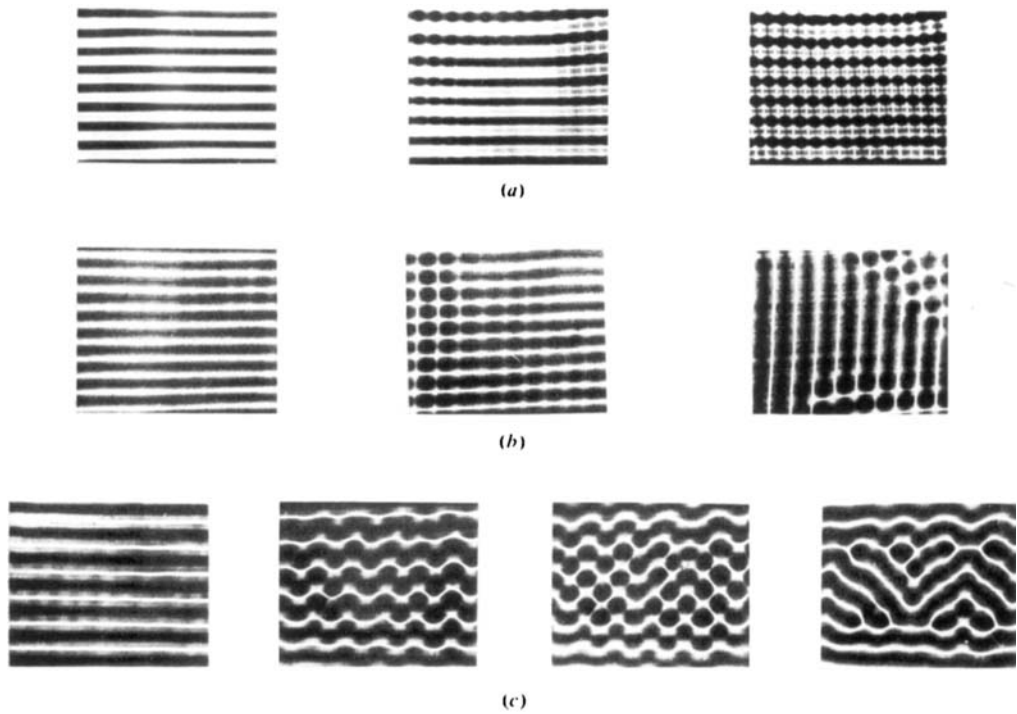


FIGURE 4. Shadowgraphs of initial rolls becoming unstable through the bimodal, cross-roll and zigzag instability. The shadowgraph at the left of each row shows the initial rolls. (a) Bimodal instability in L100 with initial wavenumber 2.95, initial $\bar{R}_a = 12460$, initial $\nu_{\max}/\nu_{\min} = 5.7$ and final $\bar{R}_a = 20500$, final $\nu_{\max}/\nu_{\min} = 10.1$. (b) Cross-roll instability in glycerine with initial wavenumber 3.98, initial $\bar{R}_a = 8400$ and initial $\nu_{\max}/\nu_{\min} = 1.75$. (c) Zigzag instability in L100 with initial wavenumber 2.42, initial $\bar{R}_a = 2900$ and initial $\nu_{\max}/\nu_{\min} = 1.8$.

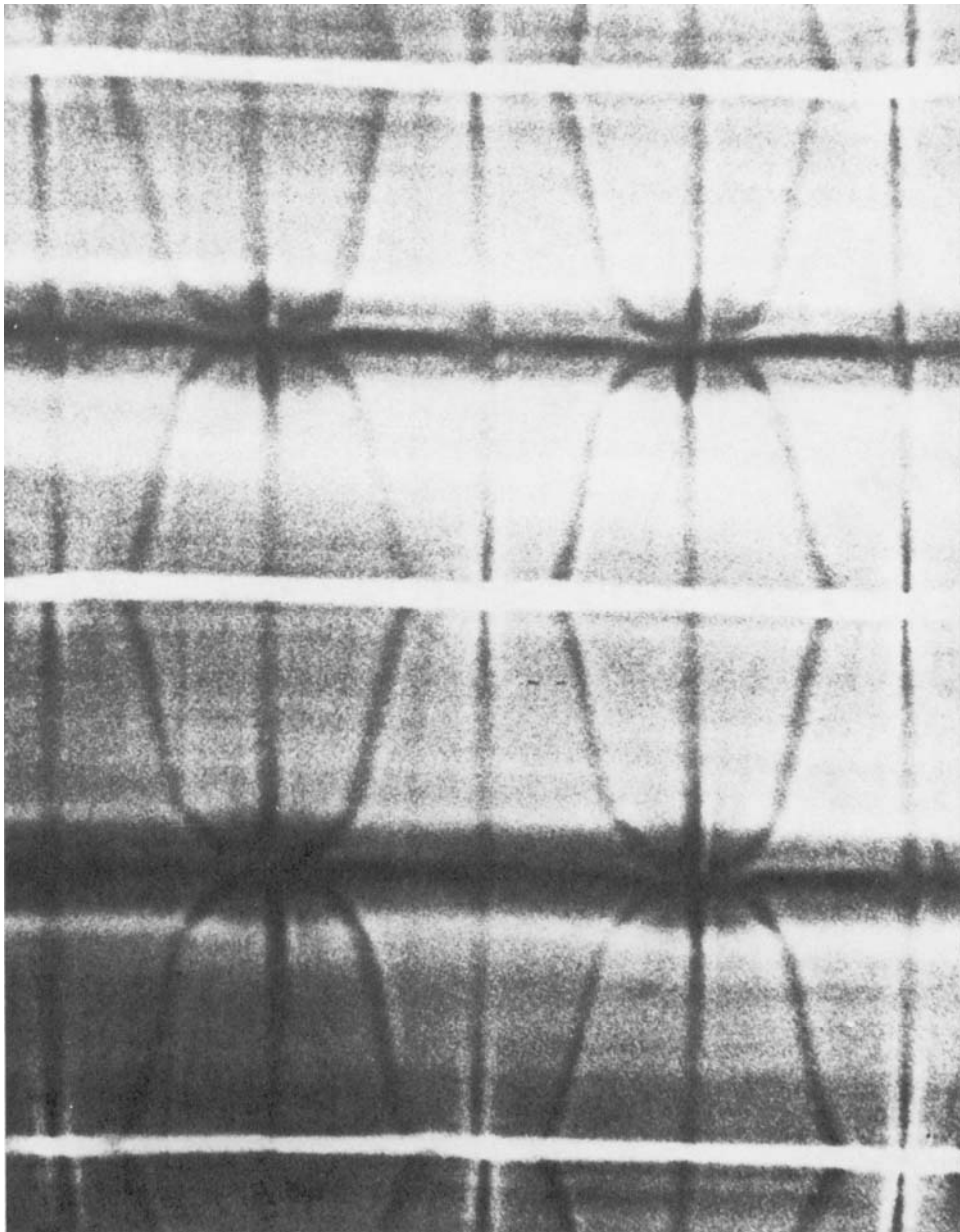


FIGURE 7. Enlargement of a shadowgraph of a weak bimodal flow in glycerine showing goblet-shaped streamlines. $\bar{R}_a = 14300$, $\nu_{\max}/\nu_{\min} = 6.5$. The streamlines are visible because of naturally occurring streaks in the glycerine that result from small amounts of water.

RICHTER